Mode locking with enhanced nonlinearity - a detailed study

Shai Yefet and Avi Pe'er[*]

Department of physics and BINA Center of nano-technology, Bar-Ilan university, Ramat-Gan 52900, Israel

[*]*avi.peer@biu.ac.il*

Abstract: We explore mode locked operation of a Ti:Sapphire laser with enhanced Kerr nonlinearity, where the threshold for pulsed operation can be continuously tuned down to the threshold for continuous-wave (CW) operation, and even below it. At the point of equality, even though a CW solution does not exist, pulsed oscillation can be realized directly from zero CW oscillation. We experimentally investigate the evolution of the mode locking mechanism towards this point and beyond it, and provide a qualitative theoretical model to explain the results.

© 2013 Optical Society of America

References and links

1. H. A. Haus, "Mode-locking of lasers," IEEE J. Sel. Top. Quantum Electron. **6**, 1173–1185 (2000).
2. T. Brabec, P. F. Curley, C. Spielmann, E. Wintner, and A. J. Schmidt, "Hard-aperture kerr-lens mode locking," J. Opt. Soc. Am. B **10**, 1029–1034 (1993).
3. H. Haken and H. Ohno, "Onset of ultrashort laser pulses: First or second order phase transition?" Opt. Commun. **26**, 117–118 (1978).
4. A. Gordon and B. Fischer, "Phase transition theory of pulse formation in passively mode-locked lasers with dispersion and kerr nonlinearity," Opt. Commun. **223**, 151–156 (2003).
5. A. Rosen, R. Weill, B. Levit, V. Smulakovsky, A. Bekker, and B. Fischer, "Experimental observation of critical phenomena in a laser light system," Phys. Rev. Lett. **105**, 013905 (2010).
6. R. Ell, U. Morgner, F. X. Kartner, J. G. Fujimoto, E. P. Ippen, V. Scheuer, G. Angelow, T. Tschudi, M. J. Lederer, A. Boiko, and B. Luther-Davies, "Generation of 5-fs pulses and octave-spanning spectra directly from a ti:sapphire laser," Opt. Lett. **26**, 373–375 (2001).
7. G. Gabetta, D. Huang, J. Jacobson, M. Ramaswamy, E. P. Ippen, and J. G. Fujimoto, "Femtosecond pulse generation in ti:al$_2$0$_3$ using a microdot mirror mode locker," Opt. Lett. **16**, 1756–1758 (1991).
8. G. P. A. Malcolm and A. I. Ferguson, "Self-mode locking of a diode-pumped nd:ylf laser," Opt. Lett. **16**, 1967–1969 (1991).
9. G. W. Pearson, C. Radzewicz, and J. S. Krasinski, "Analysis of self-focusing mode-locked lasers with additional highly nonlinear self-focusing elements," Opt. Commun. **94**, 221–226 (1992).
10. C. Radzewicz, G. W. Pearson, and J. S. Krasinski, "Use of zns as an additional highly nonlinear intracavity selffocusing element in a ti:sapphire self-modelocked laser," Opt. Commun. **102**, 464–468 (1993).
11. M. A. Larotonda, A. A. Hnilo, and F. P. Diodati, "Diode-pumped self-starting kerr-lens mode locking nd:yag laser," Opt. Commun. **183**, 485–491 (2000).
12. X. Han and H. Zeng, "Kerr-lens mode-locked ti:sapphire laser with an additional intracavity nonlinear medium," Opt. Express **16**, 18875–18880 (2008).
13. V. Magni, G. Cerullo, S. D. Silvestri, and A. Monguzzi, "Astigmatism in gaussian-beam self-focusing and in resonators for kerr-lens mode locking," J. Opt. Soc. Am. B **12**, 476–485 (1995).
14. L. Chen, M. Y. Sander, and F. X. Kartner, "Kerr-lens mode locking with minimum nonlinearity using gain-matched output couplers," Opt. Le **35**, 2916–2918 (2010).
15. M. Muller, J. Herrmann, and S. Gatz, "Kerr-lens mode locking at pump rates below continuous wave threshold," Opt. Commun. **148**, 281–284 (1998).

16. G. Fibich and A. L. Gaeta, "Critical power for self-focusing in bulk media and in hollow waveguides," Opt. Lett. **25**, 335–337 (2000).
17. V. Magni, G. Cerullo, and S. D. Silvestri, "Closed form gaussian beam analysis of resonators containing a kerr medium for femtosecond lasers," Opt. Commun. **101**, 365–370 (1993).
18. H. Kogelnik and T. Li, "Laser beams and resonators," Appl. Opt. **5**, 1550–1567 (1966).
19. H. A. Haus, J. G. Fujimoto, and E. P. Ippen, "Analytic theory of additive pulse and kerr lens mode locking," IEEE J. Quantum Electron. **28**, 2086–2096 (1992).
20. C. G. Durfee, T. Storz, J. Garlick, S. Hill, J. A. Squier, M. Kirchner, G. Taft, K. Shea, H. Kapteyn, M. Murnane, and S. Backus, "Direct diode-pumped kerr-lens mode-locked ti:sapphire laser," Opt. Express **20**, 13677–13683 (2012).

1. Introduction

The ultra-broad gain bandwidth of the Ti:Sapphire (TiS) laser renders it the 'work-horse' of the last decades for generation of ultrashort pulses by mode locking (ML) [1]. The nonlinear mechanism responsible for ML is self-focusing of the beam due to the optical Kerr effect within the TiS crystal, introducing an intensity dependent loss mechanism that favors pulses over continuous-wave (CW) operation [2]. A well known feature of ML is the abrupt transition between CW and ML operation in terms of pump power [3]. Only when the pump power crosses a certain threshold, can ML be initiated from a noise-seed (either by a knock on a cavity element or by external injection of long pulses). Another common feature is that the threshold pump power for ML is higher than the CW threshold. Typical mode locked operation requires a certain amount of CW oscillations to exist in the cavity, and only on top of the existing CW can an intensity fluctuation be amplified to create the pulse. In the following, we investigate the possibility to push the ML threshold to the extreme, i.e. the possibility of reducing the ML threshold down to the CW threshold and even lower.

The key factor for reducing the ML threshold is enhanced intracavity nonlinearity, as elegantly explained by the theory of statistical light-mode dynamics (SLD) [4]. In SLD, the mode locking procedure is transformed into a problem in statistical mechanics and the transition from CW to pulsed operation is described as a first order phase transition, which explains the threshold-like behavior of mode locking. The order parameter (analogous to temperature) is $T = N/(\gamma_s P^2)$, where N is the noise level in the cavity, γ_s represents the strength of the relevant nonlinearity and P is the total laser cavity power, that can be controlled by pump power. It was theoretically calculated that mode locking occurs below a critical value T_c of the order parameter, and it was verified experimentally in a mode locked fiber laser [5] that as the pump power increases, pulsed operation can be initiated with higher values of noise injected to the laser (for a constant nonlinear strength γ_s). Therefore, an increase in the intracavity nonlinearity will be accompanied by a decrease in the mode locking threshold.

Cavities with enhanced intracavity nonlinearity were explored in the past [6–12], showing an overall reduction of the mode locking threshold, but the limits of this phenomenon were not directly explored. In this work, we perform a detailed survey, where the Kerr nonlinearity is tuned continuously, in order to investigate the ML threshold dependence on the intracavity nonlinearity. We monitor the mode locking strength and threshold across a large parameter range and observe the optimal intracavity power for mode locking and its dependence on nonlinearity. At this optimal point, we show that with sufficiently enhanced nonlinearity, the intracavity power necessary to initiate pulsed operation can be reduced down to zero. We note that by "zero" we mean the first appearance of small CW fluctuations that experimentally identifies the threshold point, which is always smeared by noise and never completely defined.
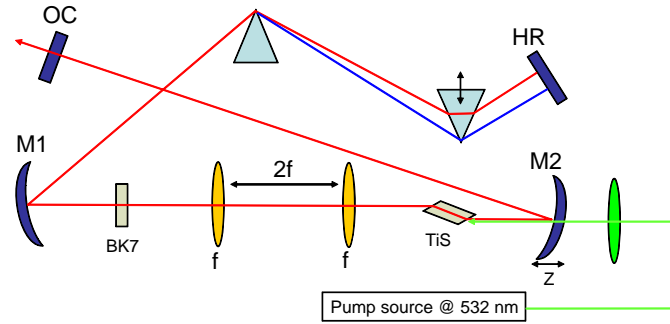
Fig. 1. Cavity configuration. The gain medium is a $3mm$ long Brewster-cut TiS crystal with 0.25 wt% doping. The curved mirrors ($M1,M2$) radius of curvature is $R = 15cm$, with high reflector (HR) and a 95% output coupler (OC) as end mirrors. An additional planar-cut BK7 window is inserted near the image point of the TiS crystal, created by the two-lens telescope of focal length $f = 10cm$. The short cavity arm is $42cm$ long and the long arm ($90cm$) contains a prism-pair of BK7 glass ($60cm$). Each cavity mirror except the OC provides group velocity dispersion of $GVD \approx -55fs^2$. The oscillator is running in the regime of anomalous dispersion.

2. Experimental setup

Our experimental setup is a standard X-fold cavity with a prism pair for dispersion compensation, as illustrated in Fig. 1. In order to enhance the intracavity nonlinearity in a controlled manner, we introduce a lens based 1x1 telescope between the curved mirrors. The focus inside the TiS crystal is thus imaged to a distance $4f$ towards mirror $M1$, where we can insert an additional planar cut Kerr medium near the imaged focus. The choice of a lens based telescope and a planar cut Kerr window (instead of the typical configuration [6] of a mirror based telescope and a Brewster cut window) is motivated by the enhanced nonlinearity and lack of nonlinear astigmatism offered by this configuration. In a Brewster cut Kerr medium the beam expands in one dimension (due to refraction) and hence the nonlinearity of the material is reduced and becomes astigmatic [13]. A planar cut Kerr medium does not suffer from beam expansion and hence the Kerr effect can be fully exploited and astigmatism free. The lens based 1x1 telescope is also astigmatism free, providing a simple expansion of the standard TiS configuration without changes of angles/mirrors (expect for some additional dispersion).

If we define δ as a measure for the distance between $M1$ and $M2$ with respect to an arbitrary reference point, we find two separate ranges of $\delta \in [\delta_1, \delta_2], [\delta_3, \delta_4]$, which allow stable CW operation of the cavity, bounded by four stability limits ($\delta_4 > \delta_3 > \delta_2 > \delta_1$). The working point for ML in our experiment is the typical working point, near the second stability limit δ_2 [2]. Near this limit, the nonlinear Kerr lensing effect causes a decrease of the mode size at the output coupler for pulsed operation compared to the CW mode size. In order to favor ML over CW operation, one can use the hard aperture technique, which can be implemented in two ways. The first is to close an aperture near the OC for a fixed value of δ. This actively induces loss on the larger CW mode, while for ML, the Kerr effect reduces the mode size, allowing the beam to pass through the aperture. Further closing the aperture will enforce pulses with higher intracavity power. The second method is to increase the distance δ between the curved mirrors beyond the stability limits, without using a physical aperture. This passively induces increasing diffraction losses on the CW mode, while the additional nonlinear Kerr lens eliminates them and stabilizes the cavity for ML. In this manner increasing the distance δ is equivalent to closing a
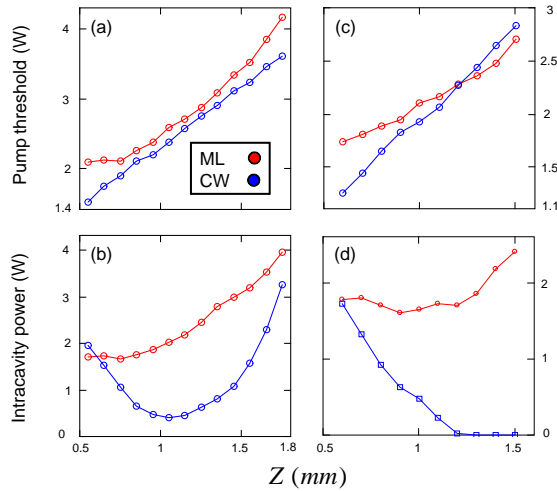
Fig. 2. ML (red) and CW (blue) operation parameters as a function of $Z = \delta - \delta_2$ for two $3mm$ long BK7 window positions: off-focus (a)+(b) and in-focus (c)+(d). Mode locking at the critical point Z_c where the ML threshold equals the CW threshold is demonstrated in the attached media file (Media 1).

physical aperture on the beam. Note that the absence of a physical aperture does not necessarily leads to the soft aperture mode locking technique. In soft aperture, a physical aperture cannot be used at the short arm, let alone to increase the curved mirror separation.

3. Results

We introduced as an additional Kerr medium a $3mm$ long planar cut window of BK7 glass. Figure 2 plots the measured ML and CW operation parameters as a function of $Z = \delta - \delta_2$. Measurements were taken for two positions of the BK7 window: 1. at the imaged focus, where considerable nonlinearity is added by the window (in-focus), 2. several centimeters away, much beyond the Rayleigh range of the intracavity mode (off-focus), where the added nonlinearity is negligible and the cavity acts as a standard TiS cavity (with some additional material dispersion). Figure 2(a) plots the CW threshold and the ML threshold as a function of Z for off-focus position. The ML threshold is defined as the minimum pump power required to initiate pulsed operation. As expected, the CW threshold increases with Z, due to increased diffraction losses (similar to closing an aperture). The ML threshold also increases (since higher power is needed for ML to overcome the loss). Figure 2(b) shows the CW and ML intracavity powers at the ML threshold as a function of Z for off-focus position. From both figures we see the typical behaviour of mode locked lasers, where the ML threshold is always larger than the CW threshold and CW oscillation must exist to initiate the ML process. In addition, although ML operation is favorable over the entire range of Z, it is most favorable at the "sweet spot" ($Z_{ss} \approx 1.1mm$), where the CW oscillation required to start the ML process reaches a minimal value, due to maximum self amplitude modulation.

The same CW and ML parameters for in-focus position are plotted in Figs. 2(c) and 2(d). The overall absolute values of the ML threshold are reduced by the added nonlinearity, and the ML threshold curve eventually crosses the CW threshold at $Z_c \approx 1.2mm$ where the intracavity CW power drops to zero. At Z_c, ML can be achieved directly from the CW threshold. The

corresponding CW and ML intracavity powers at the ML threshold are shown in Fig. 2(d), resulting in a reduction of the ML intra-cavity power as the intra-cavity nonlinearity increases. The attached Media 1 file demonstrates pulsed operation at the critical point Z_c. In the first part (spectrum), there is no signal in CW. By knocking on one of the end mirrors (we do not observe self-starting operation), an instantaneous and extremely week intensity spike is generated right at the CW threshold and immediately evolves into a pulse. In the second part (power), there is a μW signal (from crystal fluorescence), and the power jumps to $\approx 80mW$ when ML. In the third part (spatial mode), a clear circular ML mode appears on an IR card without preliminary CW mode. To verify the procedure reproducibility, the pulse is deliberately broken and re-modelocked.

Beyond the crossing point ($Z > Z_c$), ML can still be initiated, but only by first raising the pump power up to the CW threshold, locking, and then lowering the pump again. In this regime, at the CW threshold the pump power is already too high and mode locking generates a pulse with a CW spike attached to it, which can be eliminated by lowering the pump power below the CW threshold. The ML threshold in Fig. 2(c) for $Z > Z_c$ is the minimal pump power needed to maintain a clean pulse.

We can understand the need to first increase the pump power to the CW threshold and only then lower it, by noting that the CW threshold marks the crossover between decay and amplification in the cavity. For ML to occur, an intensity fluctuation must first be linearly amplified to a sufficient peak power to initiate the Kerr-lensing mechanism. For $Z > Z_c$, one must pump the laser sufficiently for a noise-induced fluctuation to be amplified (rather than decay) in order for it to reach the peak intensity required to mobilize the Kerr-lensing process. After reducing the pump power to the ML threshold, a clean pulse operation is obtained, but if ML is broken the cavity will not mode-lock again, as it does not even lase.

It is important at this point, to differentiate between the laser behaviour at $Z > Z_c$ and hysteresis effects, which are common and typical to mode locking. The hysteresis in mode locked lasers is identical to the supercooling effect in liquids. Mode locking hysteresis is the need to raise the pump power more than what is needed to sustain a pulse, in order for the laser to leave its meta-stable state and to initiate pulsed operation. Once the pulse is generated the pump power can be reduced to a lower value, but if the pulse is broken, the cavity will not mode lock again. The difference between the minimal pump power needed to initiate the pulse and the minimal pump power needed to sustain the pulse is the hysteresis gap. Hysteresis, therefore, can be observed only at $Z < Z_c$ (and was not experimentally observed in our setup). This is not the case at $Z > Z_c$, since raising the pump to the CW threshold is not because of hysteresis, but it is a necessary condition for the laser to be an amplifier at all. Below the CW threshold, the system acts as an attenuator, not an amplifier, and a meta-stable state cannot exist in the first place. Hence, this effect is inherently different from the commonly observed hysteresis loop. In this regard, our work is different from [14] where a considerable reduction of the ML threshold was achieved using a gain matched output-coupler, showing a minimum, but non-zero, CW needed to initiate pulsed operation ($7mW$ at output). Once mode locked, the pump power could be reduced even further, below the CW threshold in a hysteresis like effect, as predicted by [15].

To investigate the appearance of the regime $Z > Z_c$ for in-focus window position, we plot in Fig. 3(a)-(d) the ratio of CW to ML powers $\gamma_e \equiv P_{CW}/P_{ML}$ as a function of Z, for windows of variable thickness. γ_e represents an experimental measure for the strength of the Kerr effect, which demonstrates a "sweet spot" Z_{ss} where γ_e is minimal and the nonlinear mechanism is most efficient. The apparent tendency from Fig. 3 is that for increased nonlinearity, the γ_e value at the sweet spot is reduced and the sweet spot is pushed to larger values of Z. We find that for a $2mm$ thick window the γ_e curve touches on zero near the sweet spot, marking the onset of the new regime, where mode locking can be initiated from the CW threshold resulting
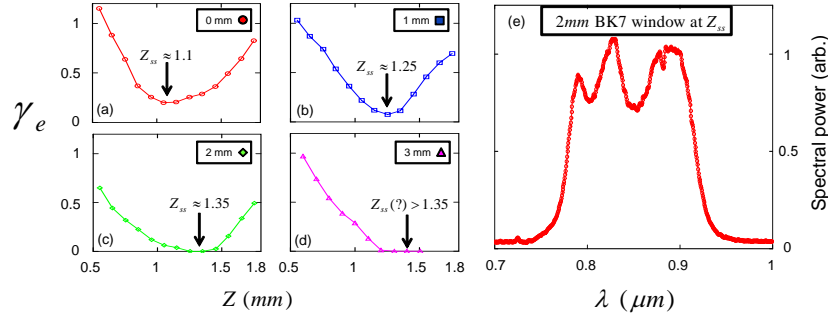
Fig. 3. (a)-(d) Experimental definition of the Kerr strength as a function of Z for BK7 window with different lengths, (e) measured spectrum for $2mm$ BK7 window at Z_{ss}.

in a pulse with energy of $\approx 30nJ$. The pulse spectrum is plotted in Fig. 3(e), resulting in a bandwidth of $\approx 140nm$ at FWHM, which corresponds to a transform-limited pulse duration of $\approx 12fs$ at FWHM. For a $3mm$ thick window the curve crosses zero at $Z = Z_c$ and the sweet-spot location Z_{ss} cannot be directly measured. Well above $Z > Z_c$ pulsed operation becomes unstable, and we could not observe the reappearance of the γ_e curve for larger values of Z. At every experimental point the prisms were adjusted to provide the broadest pulse bandwidth. The maximum oscillation bandwidth was obtained near the sweet spot due to the maximized Kerr strength, reaching approximately the same bandwidth for all of the window thicknesses used. This indicates that the bandwidth was limited mainly by high order dispersion of the prisms-mirrors combination, and not by the added dispersion of the windows. In addition, we havent seen any significant change in the mode locking starting mechanism, and pulsed operation was always started by a gentle knock on the end mirror.

4. Discussion

To provide a qualitative model for the dynamics of the "sweet spot" with increasing Kerr non-linearity we examine a commonly used theoretical measure for the Kerr Strength:

$$\gamma_s \equiv \frac{P_c}{\omega}\frac{d\omega}{dP},\tag{1}$$

where ω is the mode radius at the output coupler and P is the pulse peak power normalized to the critical power for self-focusing P_c [16]. This Kerr strength, which represents the change of the mode size due to a small increase in the ML power, is a convenient measure for mode-locking with an aperture near the output coupler. Yet, since increasing Z is equivalent to closing an aperture, γ_s is useful also for our configuration. Usually, γ_s is calculated at zero power ($P = 0$) [17] to estimate the tendency of small fluctuations to develop into pulses, however, the dependence of $\gamma_s(P)$ on power is also important. Specifically, a large (negative) value for γ_s indicates that only a small increase in the ML power (or threshold) is necessary to overcome a reduction of the aperture size (or increase in Z). The power where γ_s is most negative, represents therefore a sweet spot for mode locking. γ_s is calculated using ABCD matrices [18] and the transformed complex beam parameter [19].

Figure 4 plots $\gamma_s(P)$ for no added Kerr window (TiS only) and for a $2mm$ long added window, demonstrating a clear minimum (sweet spot) on both curves. Furthermore, as Kerr material is added (enhanced Kerr strength), the minimum point is deepened and pushed towards higher power values(larger Z), similar to the observed γ_e. Although γ_s and γ_e are somewhat differ-
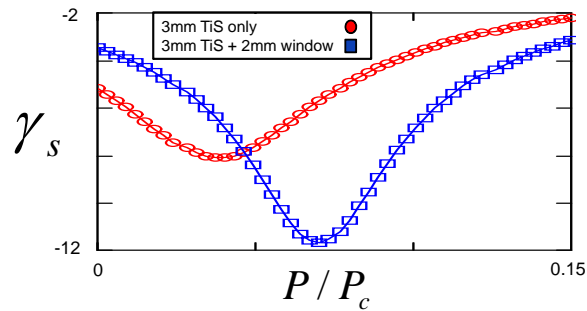
Fig. 4. Theoretical definition of the Kerr strength as a function of P for TiS crystal with added window.

ent measures for the Kerr strength, the calculation of γ_s provides reasoning for the measured behavior of the sweet spot with the different window thicknesses.

The above study of the ML threshold for varying Kerr strength provides insight to the mode locking dynamics, and an experimental verification of the critical point where ML can be initiated from zero CW power. The ML laser reported here at the critical distance Z_c, can be compared to recently published results [20] that reported a low threshold ML TiS laser with an output coupler of 99%, output power of $30mW$ and intracavity power of $3W$. Here, we have achieved ML from zero CW oscillation with similar repetition rate ($\approx 80MHz$), at much lower intracavity power and less stringent conditions. In our experiment, the output coupler had only 95% reflectivity (5 times more losses), coupling more power out ($\approx 85mW$) and considerably lower intracavity power of $1.7W$. With further optimization, the enhancement of the cavity nonlinearity may allow development of ML sources with ultra-low intra-cavity power. More importantly, our method may allow mode locked operation with high repetition rates ($> 1GHz$), which is desired for frequency comb applications. As the repetition rate is increased, the pulse energy is reduced, reaching eventually the point where pulsed operation can no longer be sustained. Increasing the intra-cavity nonlinearity can compensate for the reduction in pulse energy in lasers with high repetition rate.

Acknowledgments